

Computation of Aerodynamically Generated Sound Propagation for Aircraft Applications

Xin Zhang

with X. Chen, J. Gill, X. Huang, D. Angland, *et al.*

Airbus Aircraft Noise Technology Centre

Third International Workshop “Computational Experiment in Aeroacoustics”
September 25, 2014, Svetlogorsk, Russia

Outline of presentation

- Background
- Sound propagation problems
- Propagation methods
 - Linearised Euler Equations (LEE)
 - Gradient Term Suppression of LEE (GTS)
 - Linearised Navier-Stokes Equations (LNS)
 - Wave splitting approaches
 - Linearised Divergence Equations (LDE)
 - Gradient Term Filtering of LEE (GTF)
- Outlook
- Summary

Southampton aviation

- Eric Moon first flew from Southampton Airport site in 1910
- First transatlantic commercial service from Southampton to New York in 1939 – Pan Am Yankee Clipper



Aerospace Southampton

- Southampton Airport – 100 years continuous operation
- Seaplanes – Development & early centre
- Spitfire – Developed & manufactured
- Manpowered Flight – first successful
- Aircraft Noise Reduction
- Flight Simulation
- Sensor Systems
- Aerospace Systems Integration
- Space – Situational Awareness
- Fibre Lasers



A typical European university

- Global Students and Graduates
 - 22,000 students
 - 3,000 international
 - 100+ countries
 - 5,000 graduates each year
 - 250 degree programs
 - Over 75 different subjects
 - 150,000+ alumni
- World Leading Faculty & Staff
 - 5,000 staff
 - 200+ research groups
 - £100 million – research expenditures
- Top 20 employer in South East England
 - £billion to local economy



University aero technology centres

- Airbus Aircraft Noise Technology Centre
(<http://www.southampton.ac.uk/antc/>)
- Rolls-Royce University Technology Centre for Computational Engineering
(<http://www.soton.ac.uk/ses/research/ced/rrutc.html>)
- The Rolls-Royce University Technology Centre in Gas Turbine Noise
(<http://www.isvr.soton.ac.uk/fdag/History.HTM>)

Airbus Noise Technology Centre (ANTC)

www.southampton.ac.uk/antc

- Research support from EU, UK Government, and industry
- Close integration with Airbus R&T objectives



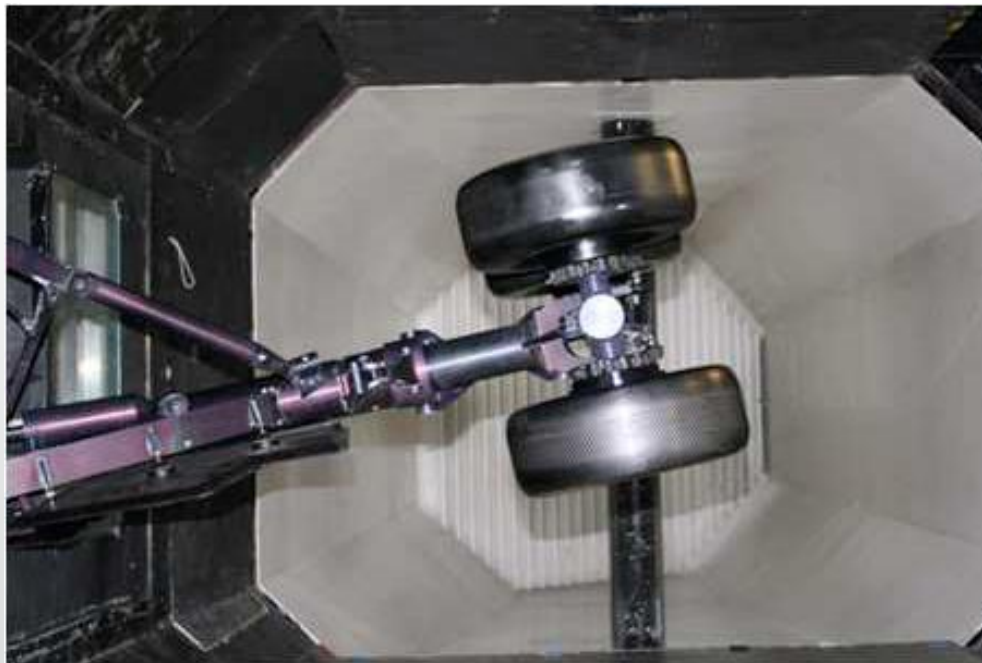
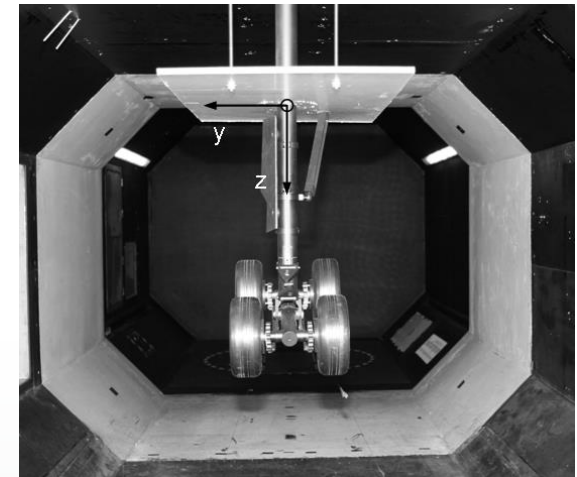
Southampton Boldrewood Innovation Campus

View of Block H with anechoic tunnel



2.1 m × 1.5 m tunnel specification

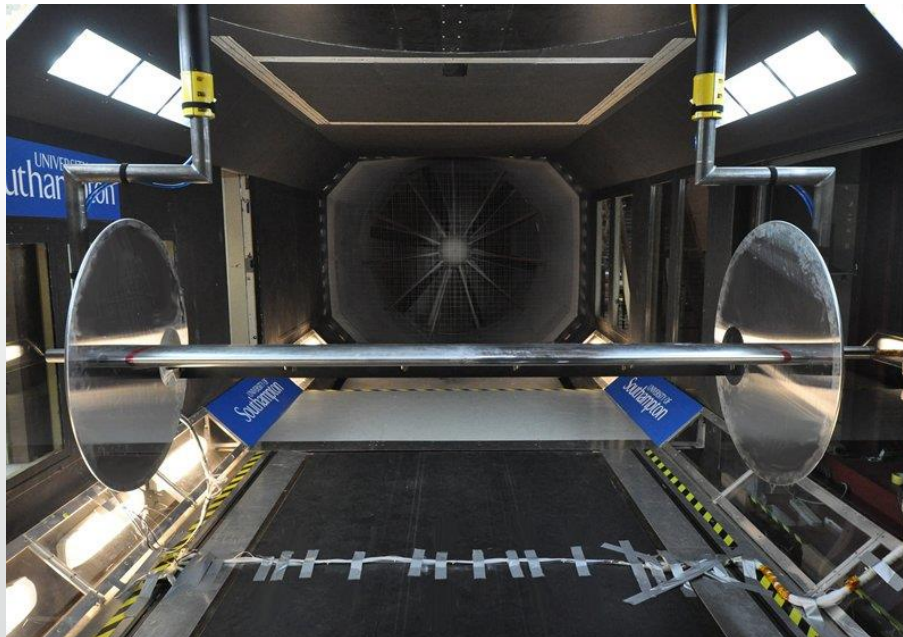
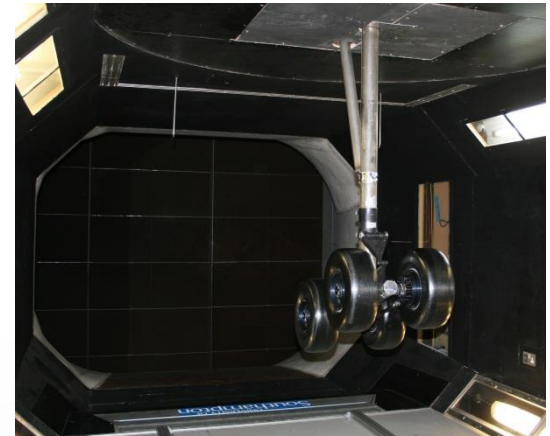
Mach Number	0.13
Maximum Flow Speed	45 m/s
Reynolds Number per metre	$3.1 \times 10^6/\text{m}$
Turbulence intensity:	<0.1% at 40 m/s
Run Time	Continuous
Test Section Size	2.1 m × 1.5 m



Closed test section, closed
circuit wind tunnel

R. J. Mitchell tunnel specification

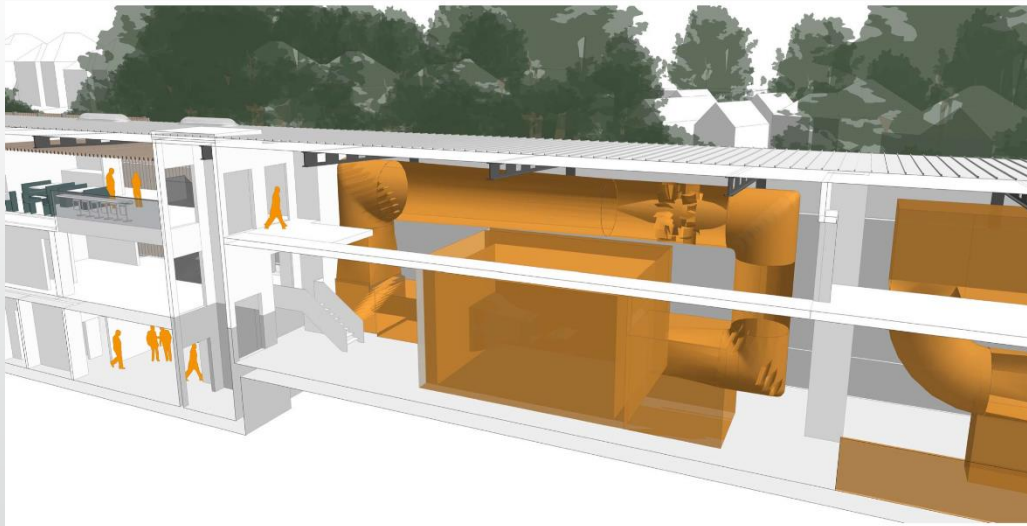
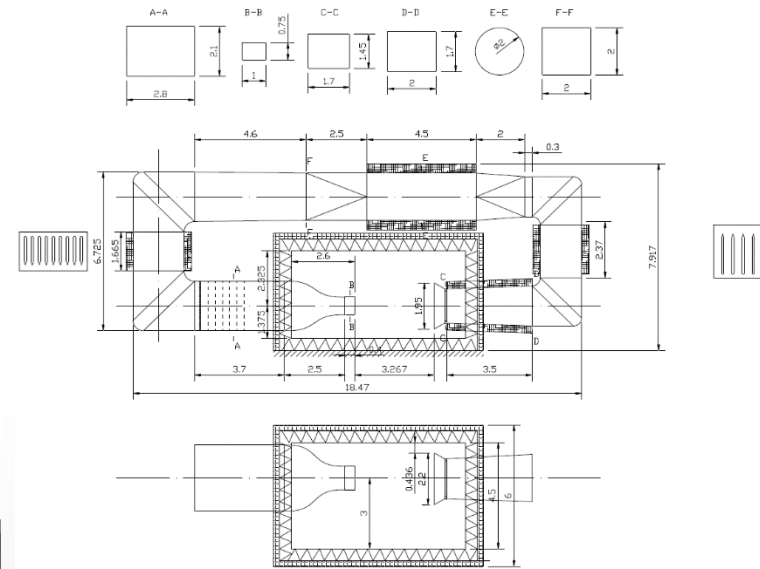
Mach Number	0.12
Maximum Flow Speed	40 m/s
Reynolds Number per metre	$2.7 \times 10^6/\text{m}$
Turbulence intensity:	<0.2% at 40 m/s
Run Time	Continuous
Test Section Size	3.5 m × 2.44 m



Closed test section, closed circuit wind tunnel incorporating temperature control

New anechoic tunnel specification

Mach Number	0.23
Maximum Flow Speed	80 m/s
Reynolds Number per metre	$5.4 \times 10^6/\text{m}$
Turbulence intensity:	TBD
Run Time	Continuous
Test Section Size	1.0 m x 0.75 m
Out of Flow Background Noise	79 dBA at 80 m/s

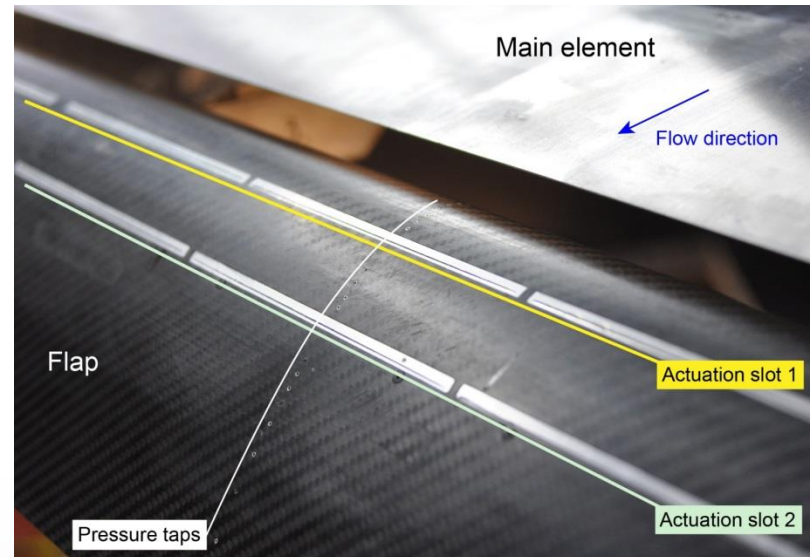
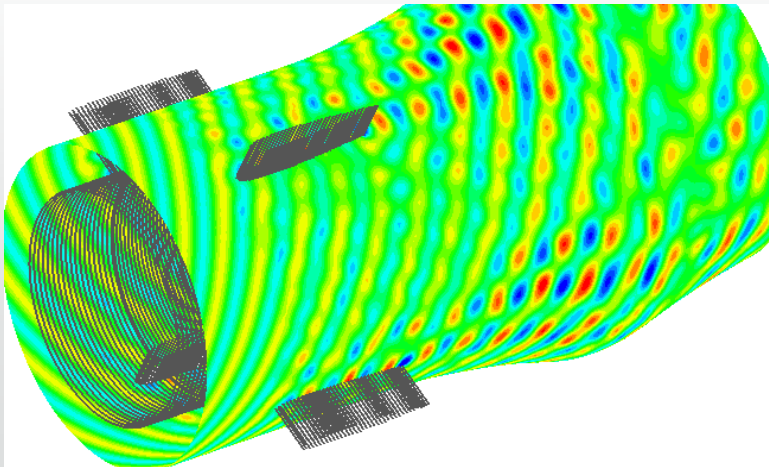


Open jet, closed circuit wind tunnel

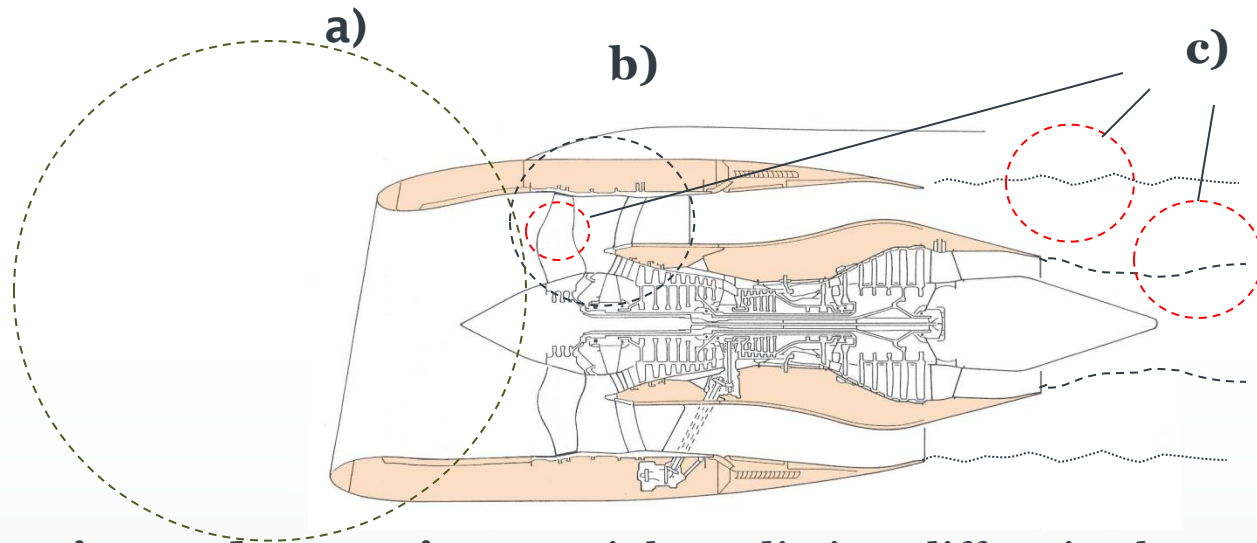
Anechoic chamber size:
8.65m x 4.65m x 5.85m

Areas of research

- Airframe noise
- Engine (turbofan and CROR) noise
- Interior noise / sound transmission
- Computational aeroacoustics
- Aerodynamics
- Aircraft noise model/predictive codes
- Noise facility/test techniques
- Flow control



Aircraft related problems



- a) **Propagation and scattering** . e.g inlet radiation, diffraction by nacelle geometry, scattering by liners, refraction by mean flow gradients, geometric spreading, far field noise prediction.
- b) **Linear interaction noise** – vortical gust(s) striking stationary or moving surfaces (e.g interaction of non-uniform inflows and wakes with blades, turbomachinery cascades ..)
- c) **Vortex generated broadband noise** fully coupled to the mean flow (e.g jet mixing noise, turbulent self noise on an airfoil/blade ..)

Possible classification

From a physical point of view, noise production and its propagation to the far field can be split into three zones:

- **Source region:** strong coupling between the aerodynamic field and acoustic field. The complete physics is nonlinear and coupled, and is described by the unsteady three-dimensional Navier-Stokes (N-S) equations.
- **Propagation region:** weak coupling between the aerodynamic field and the acoustic field. The aerodynamics flow field affects the acoustic wave propagation without feedback from the acoustic field. Sound propagation can be over an inhomogeneous / non-uniform background mean flow.
- **Radiation region:** sound radiates into the acoustic far-field, typically on a uniform background flow field. No coupling between the aerodynamics and acoustics.

Level of approximation

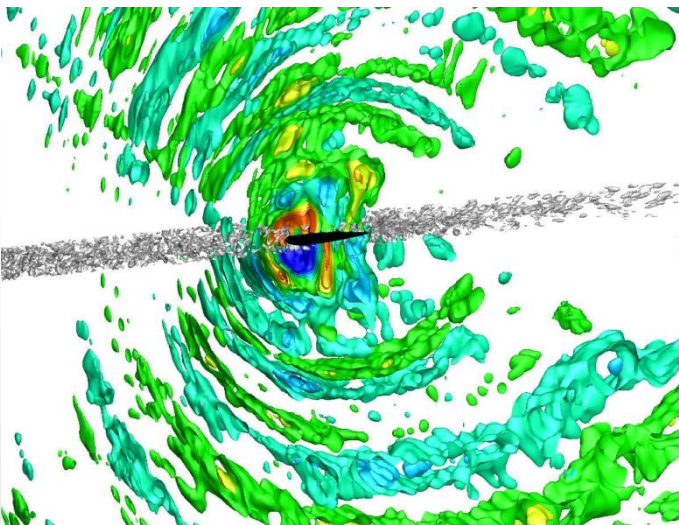
- ↓ Navier-Stokes equations
 - Complete physics but expensive...
- ↓ Full Euler equations
 - Nonlinear and treat flow and acoustic coupling and sound propagation problems together... could generate non-physical sources
- ↓ **Linearised equations**
 - Linearised about a mean-flow; can admit entropic, vortical and acoustic disturbances...
- ↓ Convected wave equations
 - Various forms, most popular form is based on velocity potential and an irrotational background mean flow assumption.

Linearised equations

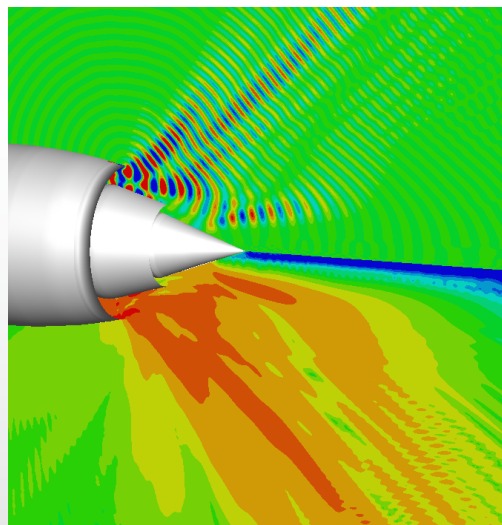
We use linearised equations because

- The magnitude of acoustic waves is normally several orders lower than its mean flow counterpart and is easily be damped. Linearisation helps maintain accurate solutions.
- Large disparity between the eddy scale l and acoustic wavelength λ . In low Mach flow the acoustic wave generation and propagation can be studied separately from the mean flow.
- The propagation effects (reflection, diffraction, *etc.*) can be directly resolved by linearised governing equations

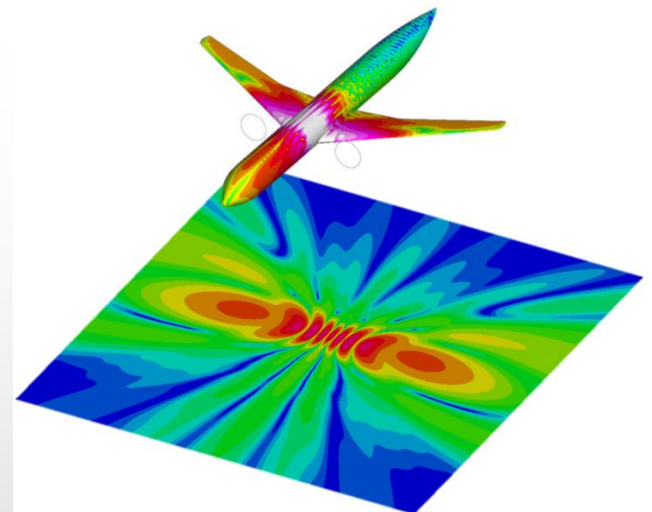
What we want to do?



Sound pressures around an airfoil using 3D synthesised turbulence



Sound propagation out of a turbofan engine bypass duct



Sound diffraction and scattering off aircraft and radiation to far-field

Some of methods that we have used so far

- **LEE** (linearised Euler equations)
- **GTS** (Gradient term suppression method)
- **LDE** (linearised divergence equations)
- **GTF** (Gradient term filtering treatment of LEE)
- **LNS** (linearised N-S equations)

Simulation tools

The ANTC has developed a suite of CFD and CAA tools, collectively known as **SotonCAA**.

Zhang, X., Chen, X.X., Morfey, C.L. and Nelson, P.A. (2004) Computation of spinning modal of radiation from an unflanged duct,” AIAA Journal, 42(9), 1795-1801.

Richards, S.K., Chen, X.X., Huang, X. and Zhang, X. (2007) Computation of fan noise radiation through an engine exhaust geometry with flow. International Journal of Aeroacoustics, 6(3), 223-241

Huang, X., Chen, X.X., Ma, Z.K. and Zhang, X. (2008) Efficient computation of spinning modal radiation through an engine bypass duct. AIAA Journal, 46(6), 1413-1423.

Ma, Z.K. and Zhang, X. (2009) Numerical investigation of broadband slat noise attenuation with acoustic liner treatment,” AIAA Journal, 47(12), 2812-2820.

Chen, X.X., Huang, X. and Zhang, X. (2009) Sound radiation from a bypass duct with bifurcations. American AIAA Journal, 47(2), 429-436

Liu, W., Kim, J.W., Zhang, X., Angland, D. and Bastien, C. (2013) Landing gear noise prediction using high-order finite difference schemes. Journal of Sound and Vibration, 332(14), 3517-3534.

Gill, J., Zhang, X. and Joseph, P. F. (2013) Symmetric airfoil geometry effects on leading edge noise. Journal of the Acoustical Society of America, 134(4), 2669-2680.

Simulation tools

SotonCAA can use the following governing equations:

- Navier-Stokes (**N-S**)
- Full Euler Equations (**FEE**)
- Linearised Euler Equations (**LEE**)
- Linearised Divergence Equations (**LDE**)
- Linearised Euler Equations with Gradient Term Filtering (**GTF**)
- Linearised Navier-Stokes (**LNS**)

Suite of codes on MPI and GPU platforms

Spatial discretisation:	<ul style="list-style-type: none"> - 6th-order prefactored compact scheme - 4th-order optimised prefactored compact scheme - 4th-order penta-diagonal scheme 	
Time integration:	<ul style="list-style-type: none"> - 4th-order RK explicit schemes - 2nd-order implicit LU-SGS scheme 	
Filtering schemes:	<ul style="list-style-type: none"> - Explicit filtering (up to 10th-order) - Adaptive non-linear artificial damping (ANAD) - 6th-order penta-diagonal filter 	
Turbulence modelling (N-S solver):	<ul style="list-style-type: none"> - Unsteady Reynolds Averaged Navier-Stokes (S-A model) - Detached-Eddy Simulation (DES/DDES/IDDES) - Large-Eddy Simulation (LES) - Zonal DES (mode I & II) 	
Boundary conditions:	<ul style="list-style-type: none"> - Solid wall (slip, non-slip, impedance) - Buffer zone - Pressure far-field - Synthesised turbulence 	
Multi-block options:	<ul style="list-style-type: none"> - One-to-one condition - Characteristic interface condition (N-S solver) 	

Linearised Euler Equations (LEE)

$$\frac{\partial p'}{\partial t} + \bar{u}_0 \cdot \nabla p' + \bar{u}' \cdot \nabla p_0 + \gamma p_0 \nabla \cdot \bar{u}' + \gamma p' \nabla \cdot \bar{u}_0 = 0,$$

$$\frac{\partial \rho'}{\partial t} + \bar{u}_0 \cdot \nabla \rho' + \bar{u}' \cdot \nabla \rho_0 + \rho_0 \nabla \cdot \bar{u}' + \rho' \nabla \cdot \bar{u}_0 = 0,$$

$$\frac{\partial \bar{u}'}{\partial t} + \bar{u}_0 \cdot \nabla \bar{u}' + \bar{u}' \cdot \nabla \bar{u}_0 + \frac{1}{\rho_0} \nabla p' - \frac{p_0}{\rho_0^2} \nabla \rho' = \bar{0},$$

Equations are derived base on assumptions:

- The background flow variables satisfy Euler equations.
- The background flow amplitudes are sufficiently larger than the disturbances.
- In terms of frequency, the background flow variables are much lower than the disturbances so they are “stationary” to the disturbances.

Acoustic, entropy, and vorticity modes

Wave analysis can be used to study linearised hyperbolic-type equations. In general, a solution of the linearised equations can be considered as a sum of three basic types of solutions

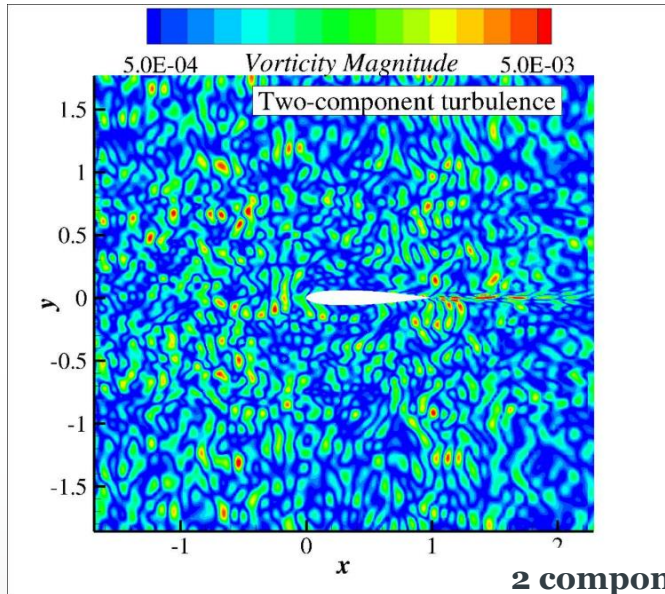
- Acoustic mode,
- Vorticity mode
- Entropy mode

The behaviours of acoustic mode and vorticity mode can be found through wave analysis. The entropy mode can generally be neglected.

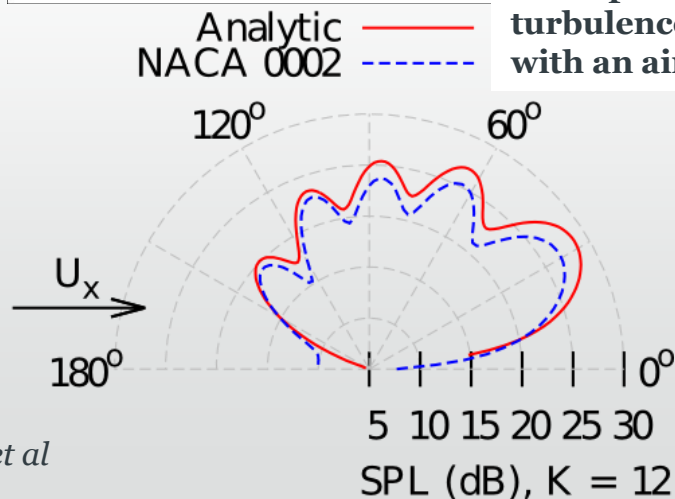
Entropy wave is produced by entropy inhomogeneities. In hyperbolic type of equations, it exists if

$$d p \neq \frac{\gamma P}{\rho} d \rho (= c^2 d \rho)$$

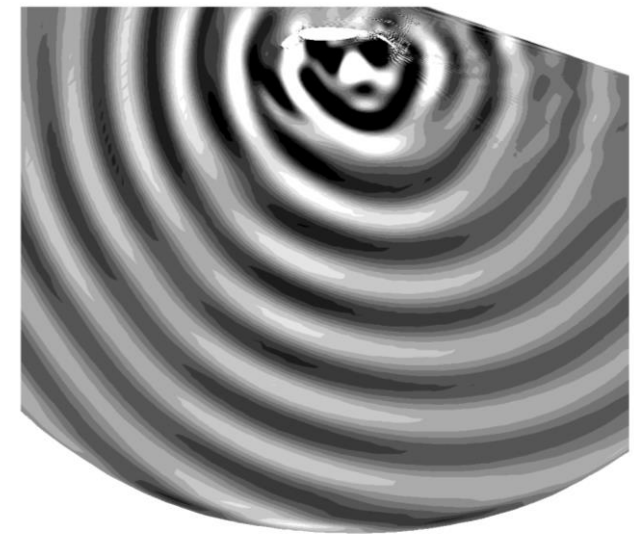
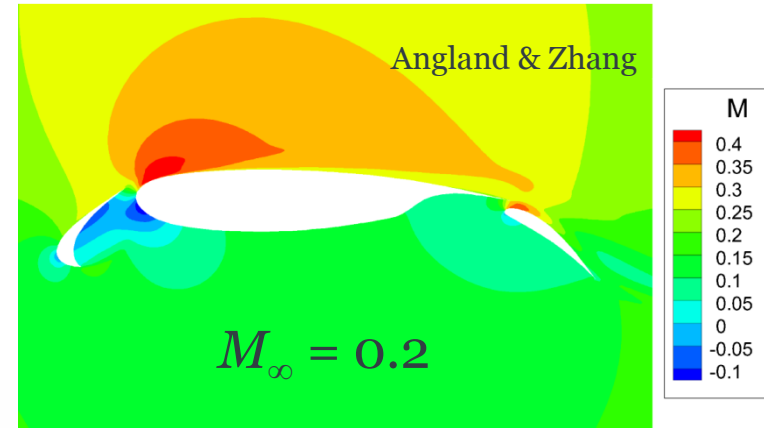
Examples of LEE computations



2 component synthesised turbulence interaction with an airfoil



Gill, *et al*



Installation effect of landing gear underneath wing and cavity

Stability issue of LEE solution

If we assume a harmonic mode expression of perturbation variables:

$$(p, \rho, u, v, w)^T = (A_p, A_\rho, A_u, A_v, A_w)^T \cdot e^{i(\omega t - k_x x - m\theta)}$$

We have, in cylindrical coordinates, the following perturbation equation:

$$\frac{d^2 A_p}{dr^2} + \left[\frac{2k_x}{\omega - k_x u_0} \frac{du_0}{dr} + \rho_0 \frac{d}{dr} \left(\frac{1}{\rho_0} \right) + \frac{1}{r} \right] \frac{dA_p}{dr} + \left[\frac{\rho_0 (\omega - k_x u_0)^2}{\gamma p_0} - k_x^2 - \frac{m^2}{r^2} \right] A_p = 0$$

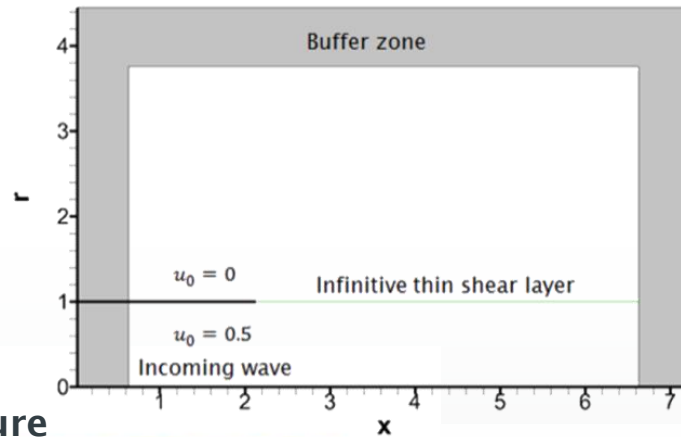
With background sheared velocity or strong density gradients, instabilities in the solution can appear.

Acoustic waves are generated by flow density compression and expansion. They have no connection to vortical and entropy waves, although they are affected by instabilities.

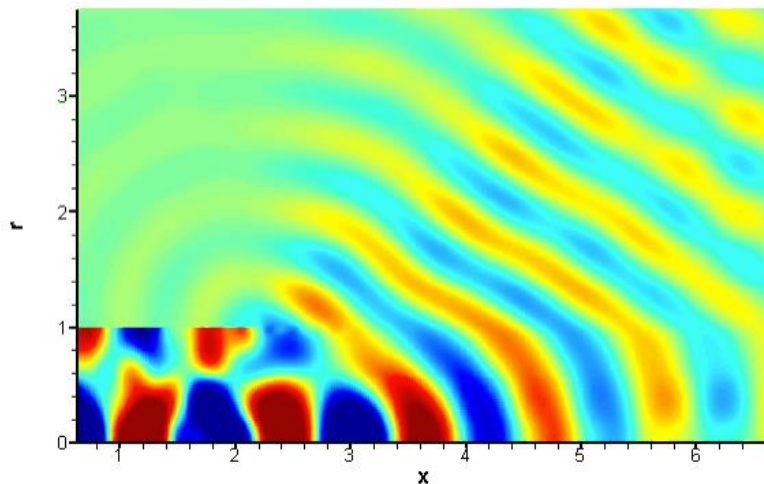
For stable acoustic wave simulation a possible solution is to separate the acoustic waves from the others via a wave-splitting method.

Illustration of acoustic and vorticity waves

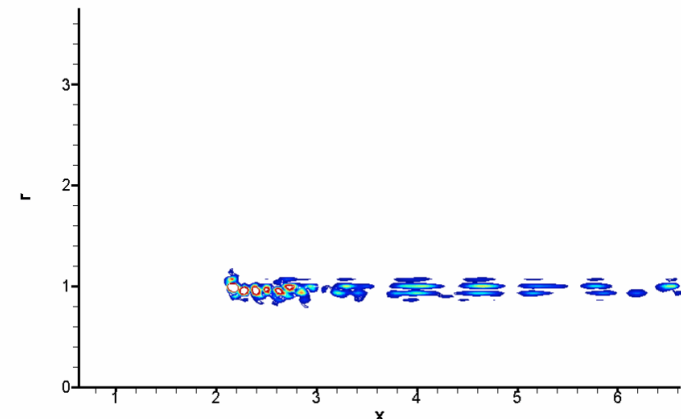
Modal propagation in and radiation out of a semi-infinite duct, mode (0,1), frequency = 500 Hz



Pressure



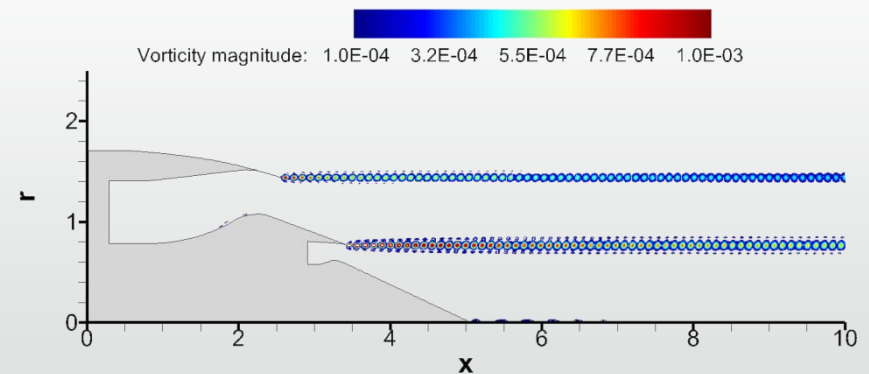
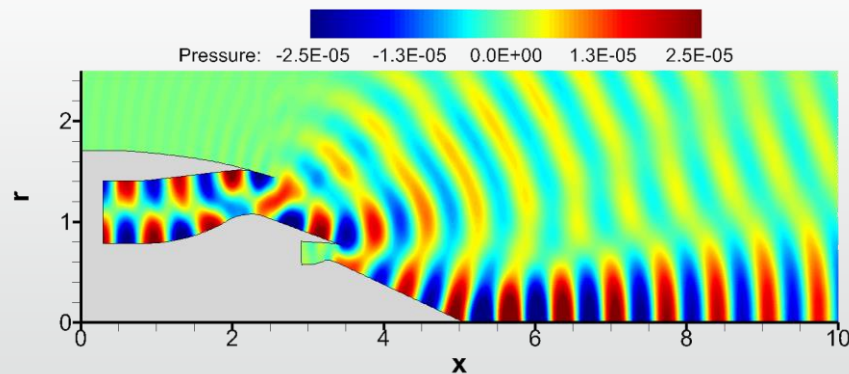
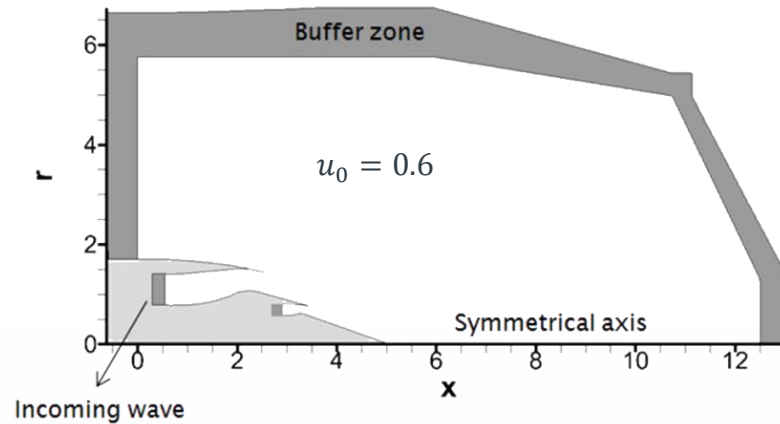
Vorticity



Instability waves and vortical modes

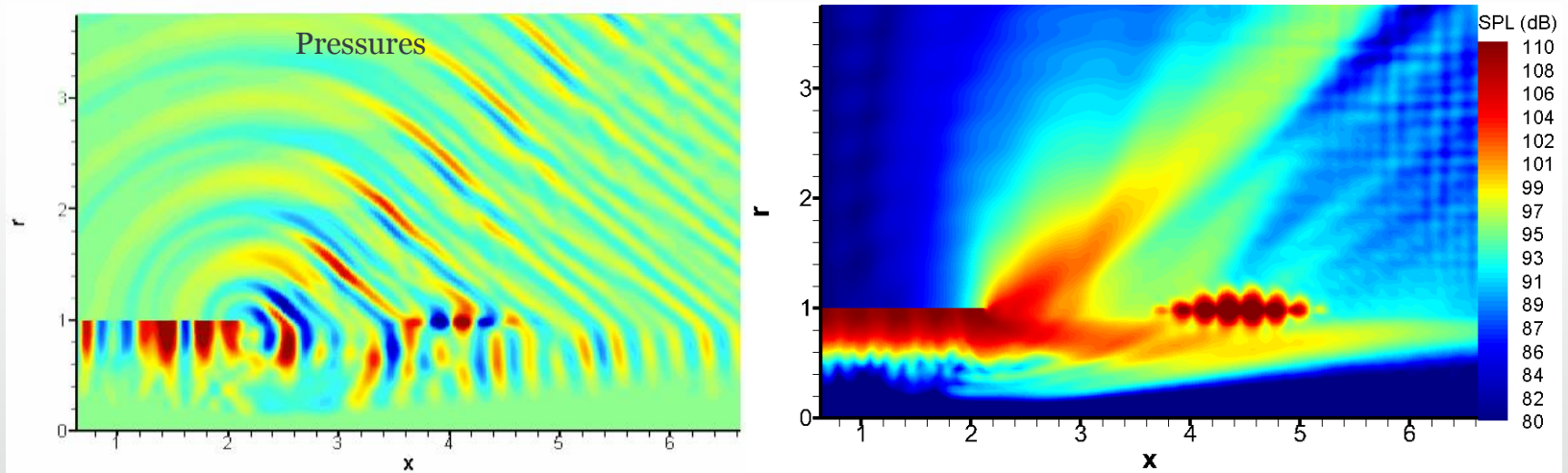
- The vorticity mode results in instability waves. The instability waves (perturbed vorticity) can be induced either by acoustic waves crossing **shear layers** or by acoustic waves encountering **geometric discontinuities**.
- In terms of sheared flow, the problem can be associated with Kelvin-Helmholtz instability. In linear stability theory, a system of parallel shear flows can be absolutely or convectively unstable. A convectively unstable flow can be globally unstable only if there are spatially growing waves at the excitation acoustic frequency.

Modal radiation from an engine bypass duct



Linearised Euler equations

LEE would fail when simulating a convectively unstable hydrodynamic-acoustic system when the spatially growing instability waves are generated by **steady periodic forcing** in the range of **unstable frequencies**. As shown in the figure below, the perturbed pressure field is clearly impacted by a growing vorticity wave.



Mode (6,1), including 4 individual frequencies 500Hz, 1000 Hz, 1500Hz and 2000Hz.

Gradient term suppression (GTS) LEE

$$\frac{\partial \rho'}{\partial t} + \frac{\partial(\rho' u_0 + \rho_0 u')}{\partial x} + \frac{\partial(\rho' v_0 + \rho_0 v')}{\partial y} + \frac{\partial(\rho' w_0 + \rho_0 w')}{\partial z} = 0,$$

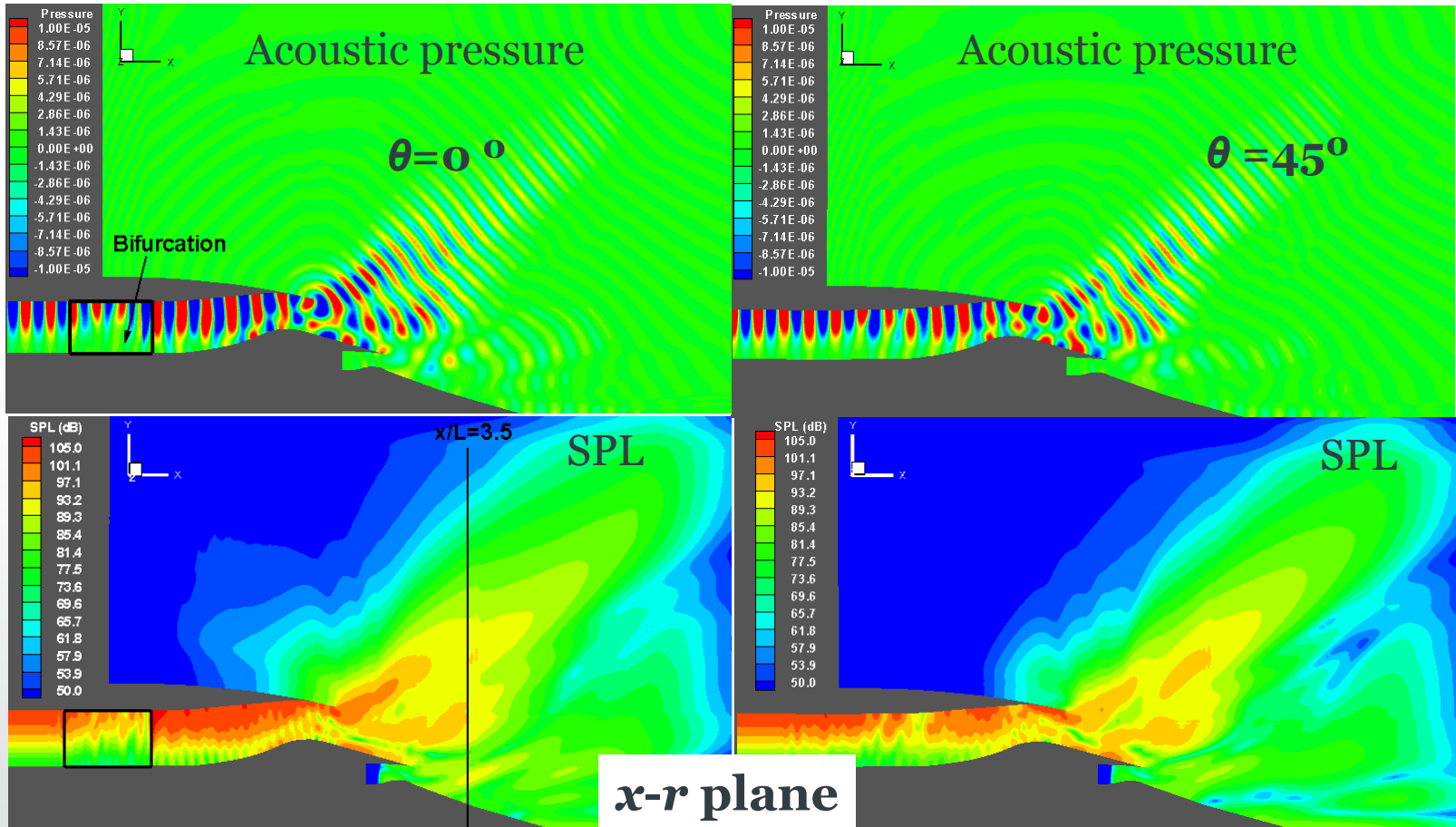
$$\frac{\partial u'}{\partial t} + u_0 \frac{\partial u'}{\partial x} + v_0 \frac{\partial u'}{\partial y} + w_0 \frac{\partial u'}{\partial z} + u' \frac{\partial u_0}{\partial x} + v' \frac{\partial u_0}{\partial y} + w' \frac{\partial u_0}{\partial z} + \frac{\partial p'}{\rho_0 \partial x} - \frac{\rho' \partial p_0}{\rho_0^2 \partial x} = 0,$$

$$\frac{\partial v'}{\partial t} + u_0 \frac{\partial v'}{\partial x} + v_0 \frac{\partial v'}{\partial y} + w_0 \frac{\partial v'}{\partial z} + u' \frac{\partial v_0}{\partial x} + v' \frac{\partial v_0}{\partial y} + w' \frac{\partial v_0}{\partial z} + \frac{\partial p'}{\rho_0 \partial y} - \frac{\rho' \partial p_0}{\rho_0^2 \partial y} = 0,$$

$$\frac{\partial w'}{\partial t} + u_0 \frac{\partial w'}{\partial x} + v_0 \frac{\partial w'}{\partial y} + w_0 \frac{\partial w'}{\partial z} + u' \frac{\partial w_0}{\partial x} + v' \frac{\partial w_0}{\partial y} + w' \frac{\partial w_0}{\partial z} + \frac{\partial p'}{\rho_0 \partial z} - \frac{\rho' \partial p_0}{\rho_0^2 \partial z} = 0.$$

Term associated with mean velocity gradient are ignored.

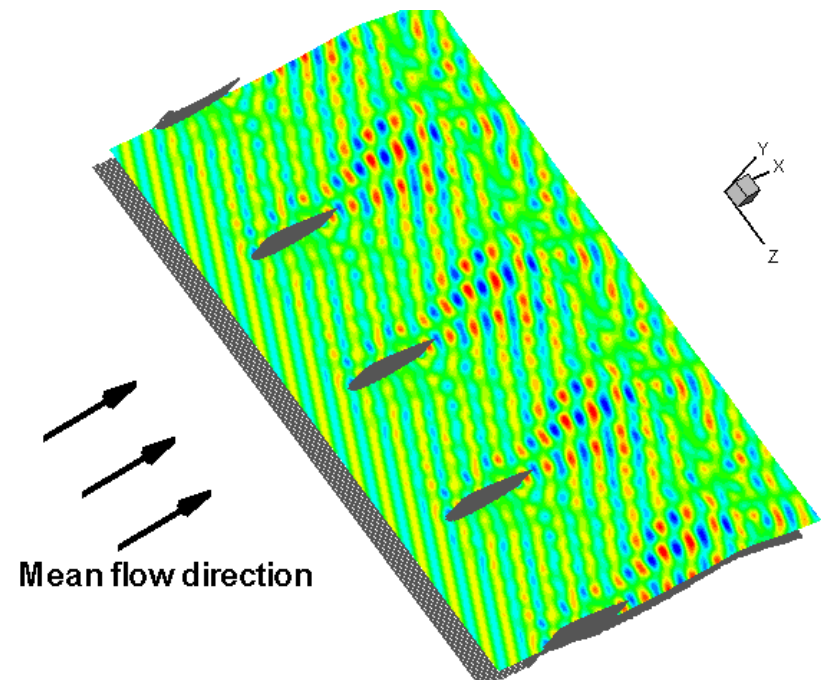
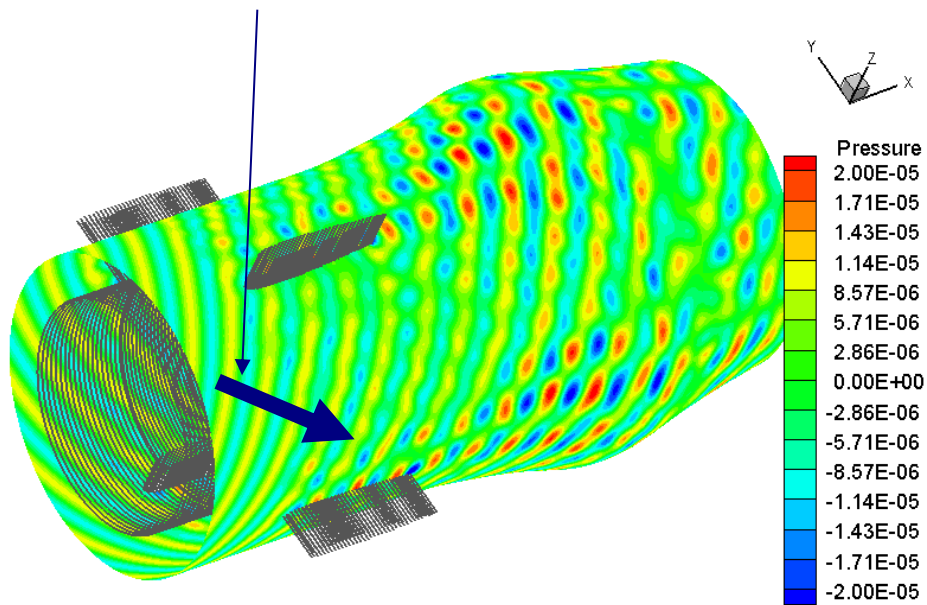
Mode radiation out of an engine bypass duct



Single mode at $m=12, n=1, f=1545$ Hz ($k=28$)

With bifurcation inside duct

Spinning mode moving direction



Radial index $J=20$ ($r=1.1 \sim 1.28$ m)

Plane view

x - θ plane

Divergence equations

The acoustic-mode velocity is curl-free. On the basis of Helmholtz's theorem, the irrotational and solenoidal components of velocity can be split into independent parts, respectively the acoustic part (ignoring entropy effects) and the vortical part, as follows,

$$\vec{u} = \nabla\phi + \nabla \times \vec{\psi}$$

The acoustical velocity ($\nabla\phi$) is curl-free and can be obtained by applying a divergence operator to momentum equation

- A velocity potential equation is derived using divergence velocity components
- A divergence operator is used to obtain curl-free flow data
- Mean flow density gradient is accounted for.

Divergence equations

Starting from vector form of momentum equations

$$\frac{\partial \vec{u}}{\partial t} + (\vec{u} \cdot \nabla) \vec{u} + \frac{\nabla p}{\rho} = 0$$

Taking the divergence operator on the equation above, we have:

$$\frac{\partial \nabla \cdot \vec{u}}{\partial t} + \nabla \cdot [(\vec{u} \cdot \nabla) \vec{u}] + \nabla \cdot \left(\frac{\nabla p}{\rho} \right) = 0$$

Let $\delta = \nabla \cdot \vec{u}$, we have

$$\frac{\partial \delta}{\partial t} + \vec{u} \cdot \nabla \delta + \frac{\partial \vec{u}}{\partial x} \cdot \nabla u + \frac{\partial \vec{u}}{\partial y} \cdot \nabla v + \frac{\partial \vec{u}}{\partial z} \cdot \nabla w + \nabla \cdot \left(\frac{\nabla p}{\rho} \right) = 0$$

Divergence equations

We can now write an alternative form of divergence equation as

$$\frac{\partial \delta}{\partial t} + \nabla \cdot \left(\vec{u} \delta + \frac{\nabla p}{\rho} \right) - 2\Phi = 0$$

where

$$\delta = \nabla \cdot \vec{u} = \frac{\partial u}{\partial x} + \frac{\partial v}{\partial r} + \frac{\partial w}{\partial z} = \nabla^2 \phi,$$

$$\Phi = \frac{\partial u}{\partial x} \frac{\partial v}{\partial y} - \frac{\partial v}{\partial x} \frac{\partial u}{\partial y} + \left(\frac{\partial u}{\partial x} + \frac{\partial v}{\partial y} \right) \frac{\partial w}{\partial z} - \frac{\partial v}{\partial z} \frac{\partial w}{\partial y} - \frac{\partial u}{\partial z} \frac{\partial w}{\partial x}$$

Divergence equations

Final form:

$$\frac{\partial \phi}{\partial t} + \frac{p}{\rho} + \varphi_2 = 0$$

where

$$\nabla^2 \varphi_2 = \nabla \cdot \left(\vec{u} \delta - \frac{p}{\rho^2} \nabla \rho \right) - 2\Phi$$

Linearised Divergence equations (LDE)

Finally LDE can be obtained through a linearisation process

$$\frac{\partial \rho'}{\partial t} + \vec{u}_0 \cdot \nabla \rho' + u' \cdot \nabla \rho_0 + \rho_0 \delta' + \delta_0 \rho' = 0,$$

$$\frac{\partial \phi'}{\partial t} + \frac{p'}{\rho_0} + \varphi_2 = 0,$$

where

$$p' = c_0^2 \rho', \quad (c_0^2 = \mathcal{P}_0 / \rho_0)$$

$$\nabla^2 \varphi_2 = \nabla \cdot \left(\vec{u}_0 \delta' + \vec{u}' \delta_0 - \frac{p'}{\rho_0^2} \nabla \rho_0 - \frac{p_0}{\rho_0^2} \nabla \rho' \right) = \mathbf{E},$$

$$\delta' = \nabla^2 \phi', \quad u' = \nabla \phi'$$

Linearised Divergence equations (LDE)

The Poisson equation involving φ_2 is solved through an iterative process.

For uniform mean flow the above equation has a simple solution

$$\varphi_2 = \vec{u}_0 \cdot \vec{u}' = u_0 u' + v_0 v' + w_0 w'$$

Therefore at physical boundaries such as slip-walls, this simple solution can be used to obtain the value of φ_2 by assuming uniform mean flow.

At the inner block boundary (called one-to-one boundary) the value of φ_2 is constantly updated using its value nearby before solving the Poisson equation. Normally the convergence can be reached within an iterative number of 10.

Linearised Divergence equations (LDE)

LDE solution procedure:

- Solving Poisson equation for φ_2 : $\nabla^2 \varphi_2 = \nabla \cdot \left(\vec{u}_0 \delta' + \vec{u}' \delta_0 - \frac{p'}{\rho_0^2} \nabla \rho_0 - \frac{p_0}{\rho_0^2} \nabla \rho' \right),$
- Calculation of tendency term: $\frac{\partial \phi'}{\partial t} = -\frac{p'}{\rho_0} - \varphi_2$
- Calculation of velocity vector: $\vec{u}' = \nabla \phi'$

Gradient term filtering (GTF)

GTF is introduced in order to include vortical modes. It keeps the form of LEE.

- The time tendency term $\partial \vec{u}' / \partial t$ of the momentum equation, which is a summation of all gradient terms, contains acoustic and vortical modes.
- This term is filtered using a divergence operator and a curl operator to extract information about acoustic and vortical modes.
- A new time tendency term is recovered

$$\frac{\partial \vec{u}'}{\partial t} = \nabla \cdot \frac{\partial \phi'}{\partial t} + \nabla \times \frac{\partial \vec{\psi}'}{\partial t}$$

as a replacement in the LEE solving procedure.

Gradient term filtering (GTF)

In practical implementations an equivalent procedure is adapted. The operators are applied to the velocity vector \vec{u}' at time level n instead of its time tendency $\partial\vec{u}' / \partial t$.

Since the velocity vector at time level $n-1$ has already been filtered, it is sufficient to filter only the velocity vector at time level n to ensure stability.

- GTF is solved in Euler form with the concept of wave-splitting.
- GTF is stable for acoustic wave simulation
- For vortex sound, GTF is stable for many applications, such as sound propagating through a sheared flow.

Gradient term filtering (GTF)

GTF solution procedure:

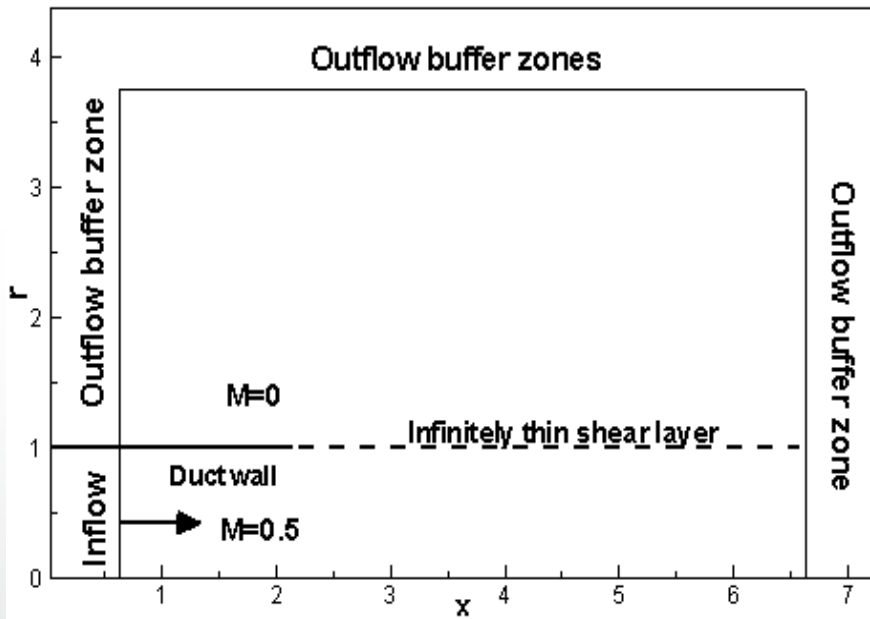
- Solving Poisson equation for ϕ' and $\vec{\psi}'$ from \vec{u}'
- Calculation of velocity vector: $\vec{u}'_* = \nabla \cdot \phi' + \nabla \times \vec{\psi}'$
- LEE computation:

$$\frac{\partial p'}{\partial t} = -\vec{u}_0 \cdot \nabla p' - \vec{u}'_* \cdot \nabla p_0 - \gamma p_0 \nabla \cdot \vec{u}'_* - \gamma p' \nabla \cdot \vec{u}_0,$$

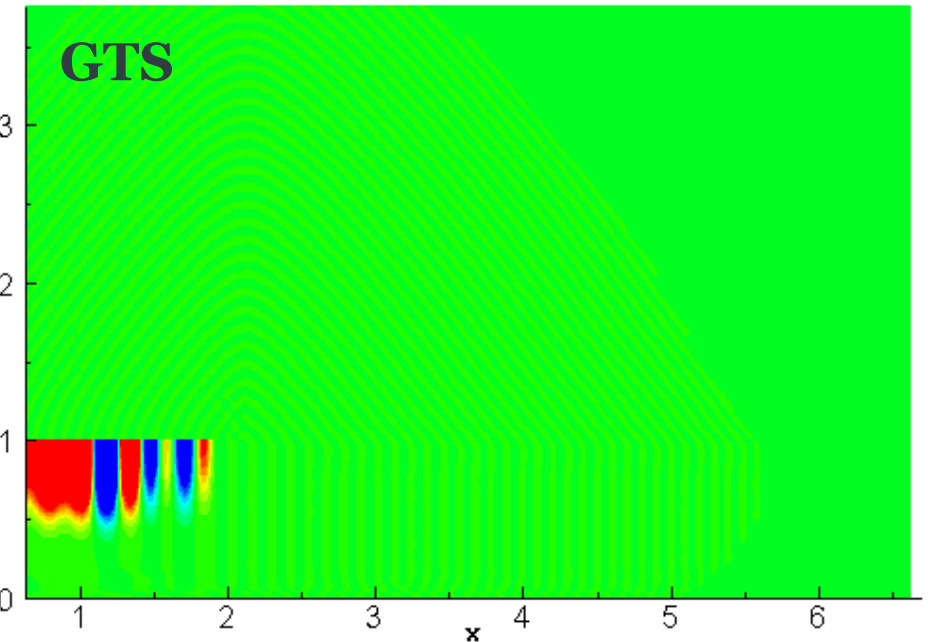
$$\frac{\partial \rho'}{\partial t} = -\vec{u}_0 \cdot \nabla \rho' - \vec{u}'_* \cdot \nabla \rho_0 - \rho_0 \nabla \cdot \vec{u}'_* - \rho' \nabla \cdot \vec{u}_0,$$

$$\frac{\partial \vec{u}'}{\partial t} = -\vec{u}_0 \cdot \nabla \vec{u}'_* - \vec{u}'_* \cdot \nabla \vec{u}_0 - \frac{1}{\rho_0} \nabla p' + \frac{p_0}{\rho_0^2} \nabla \rho'$$

Modal radiation from an unflunged duct



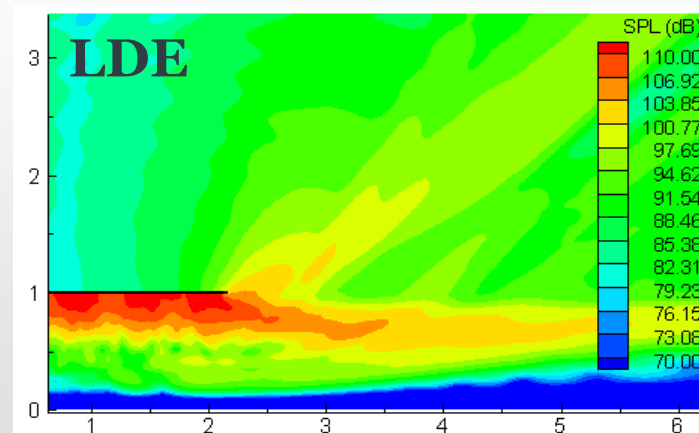
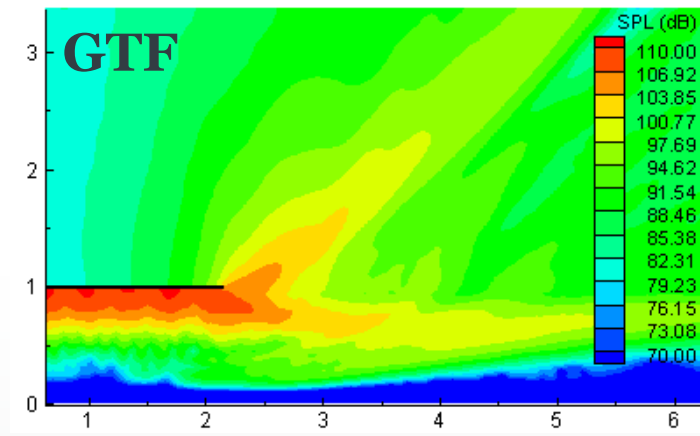
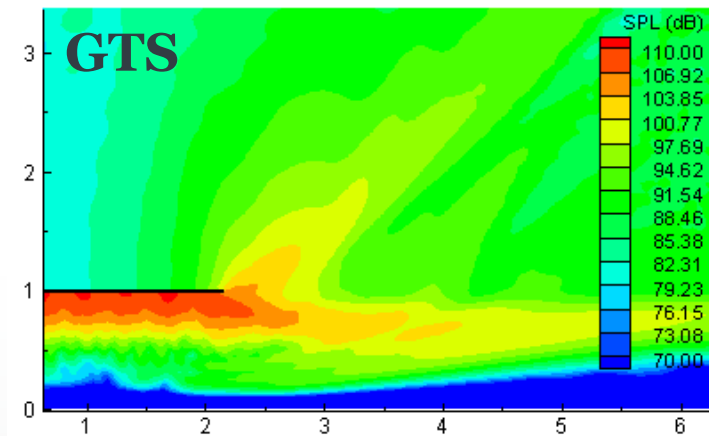
Computational domain



Animation (acoustic pressure contours)

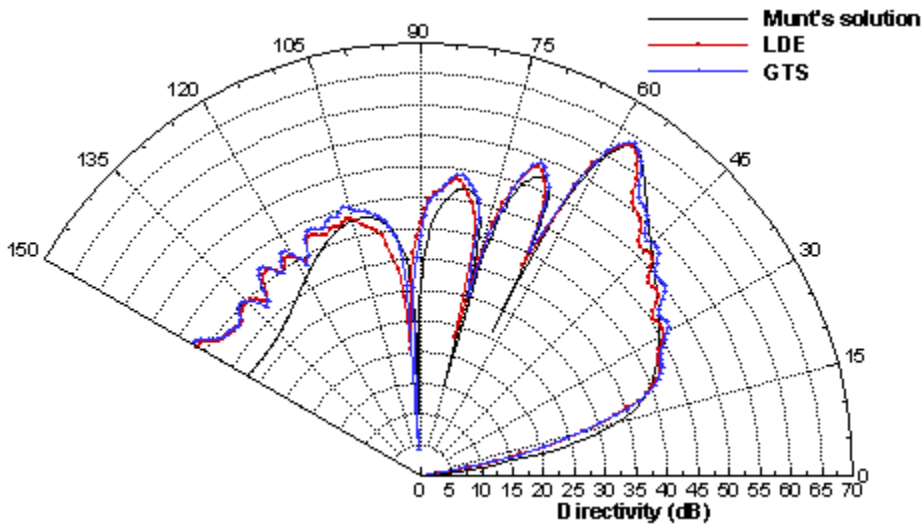
Mode $(m,n)=(6,1)$; Four frequencies combination: $f=500,1000,1500,$ and 2000Hz

Near-field predictions

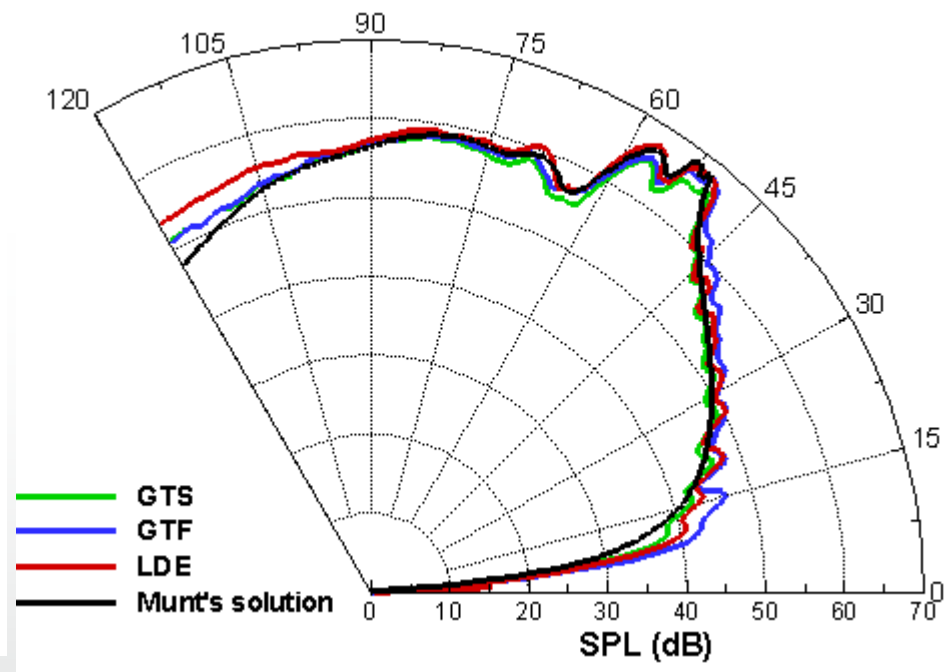


Near-field sound pressure contours

Far-field directivity



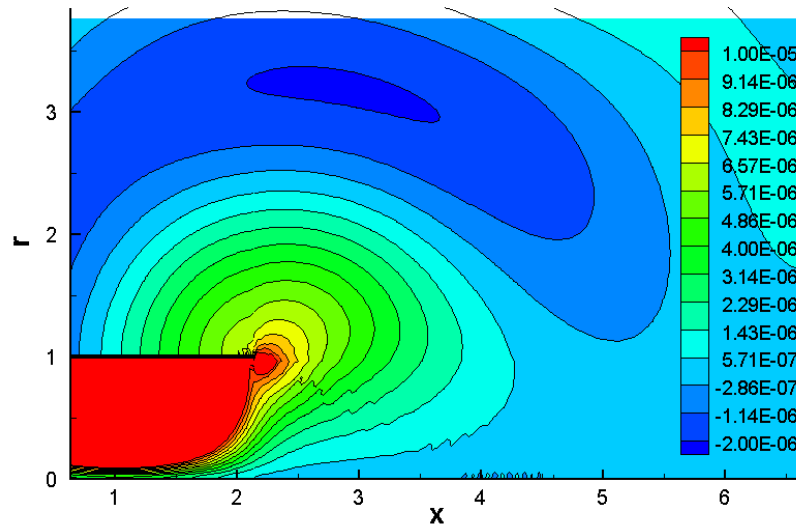
Single frequency at 1000 Hz



4 frequencies from 500 to 2000 Hz

Further tests

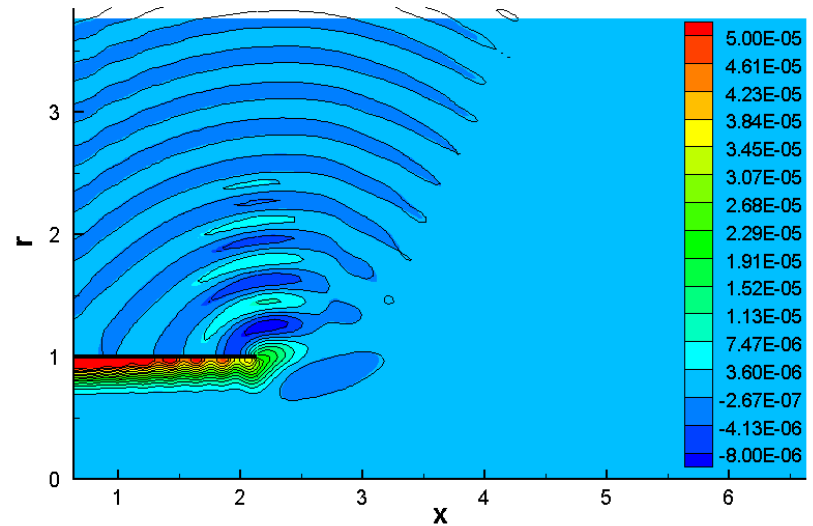
Near-field acoustic pressure



Mode (1,1), frequency = 100Hz
Cut-on ratio = 1.158

Low frequency, low cut-on ratio

Near-field acoustic pressure

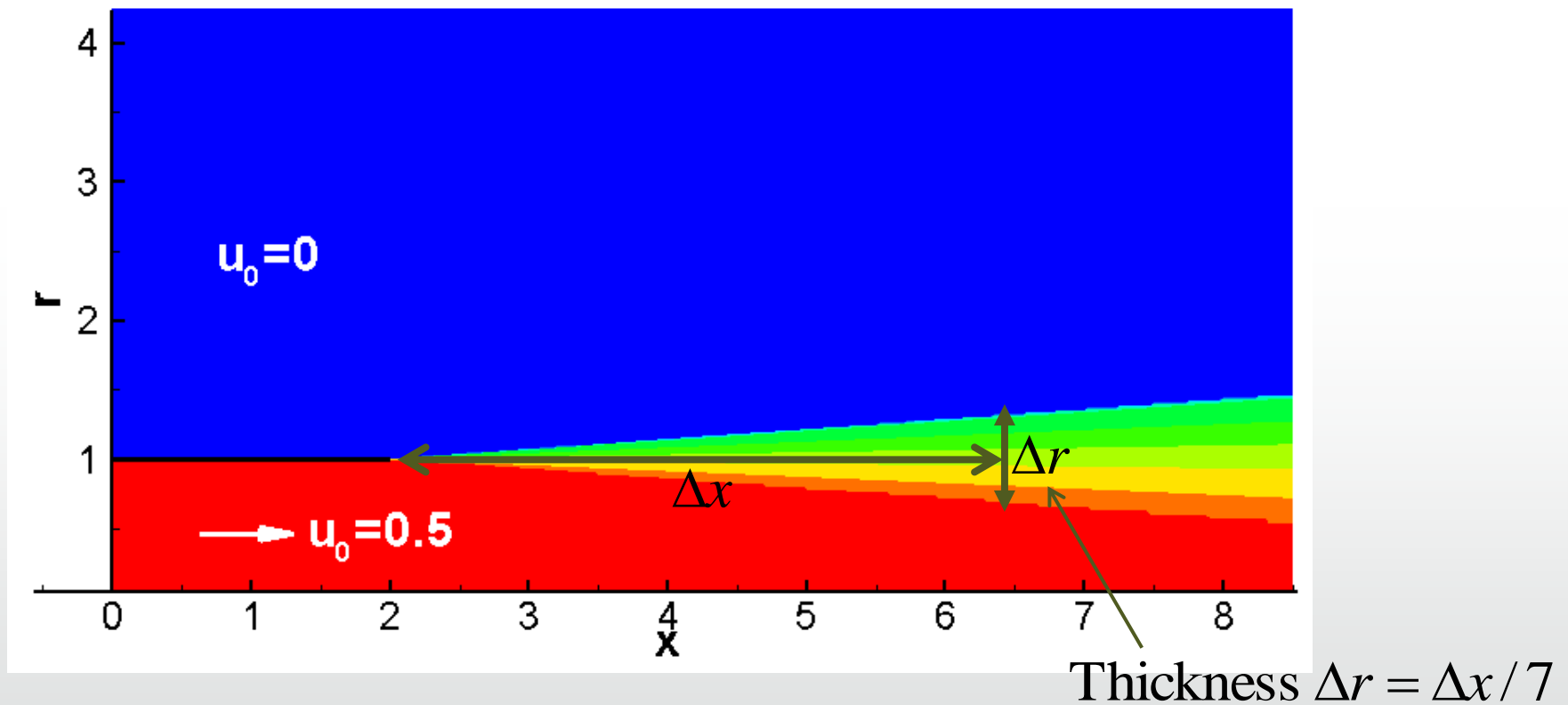


Mode (20,1), frequency = 1210Hz
Cut-on ratio = 1.161

High frequency, low cut-on ratio

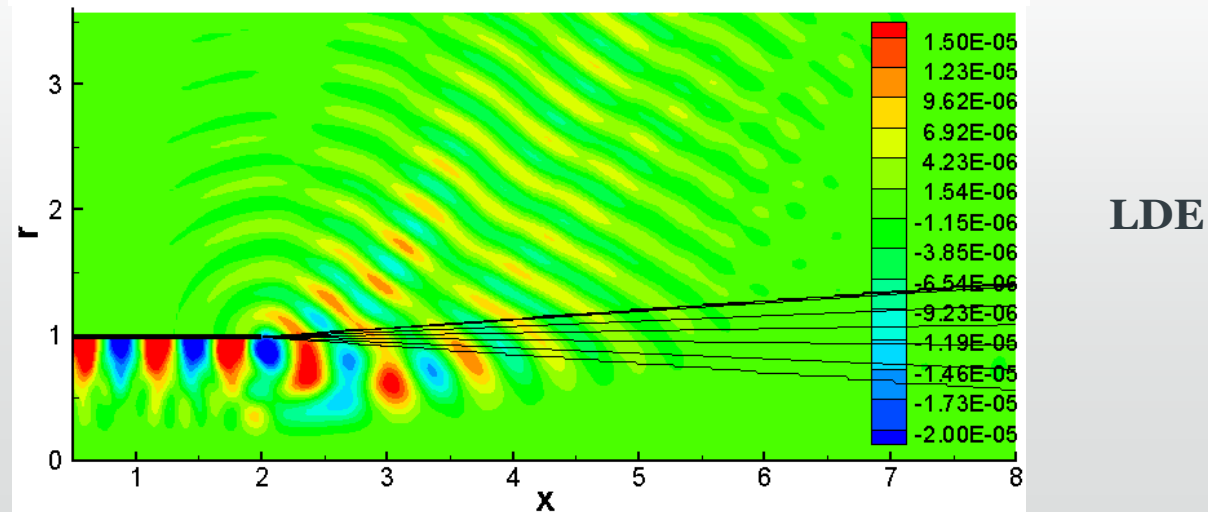
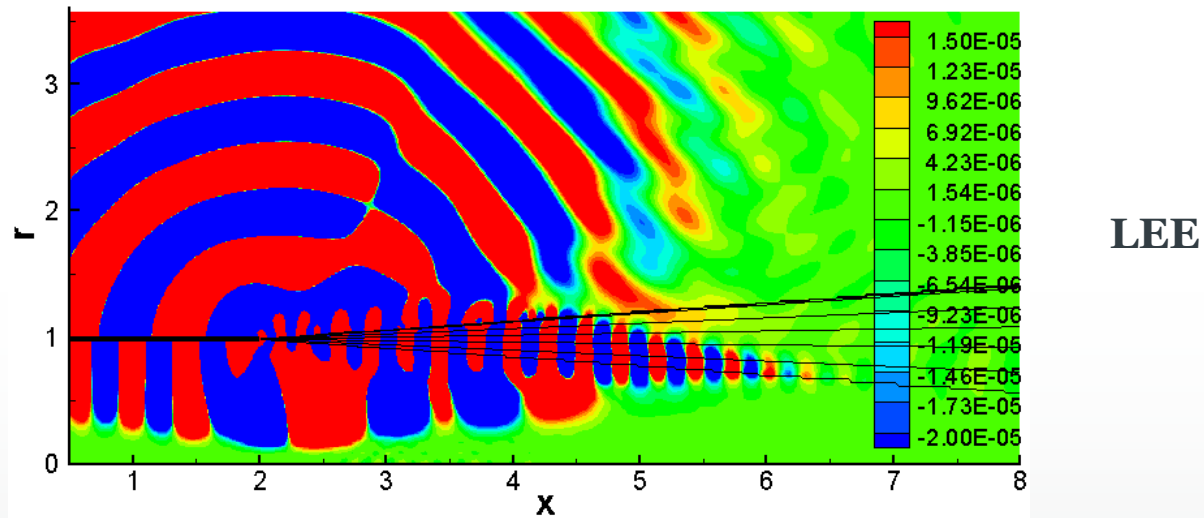
Further LDE test: linear shear layer

Shear velocity profile: $u_0(r) = 0.25[1 - \text{erf}(\Delta r)]$, and error function $\text{erf}(r) = \frac{2}{\sqrt{\pi}} \int_0^r e^{-t^2} dt$



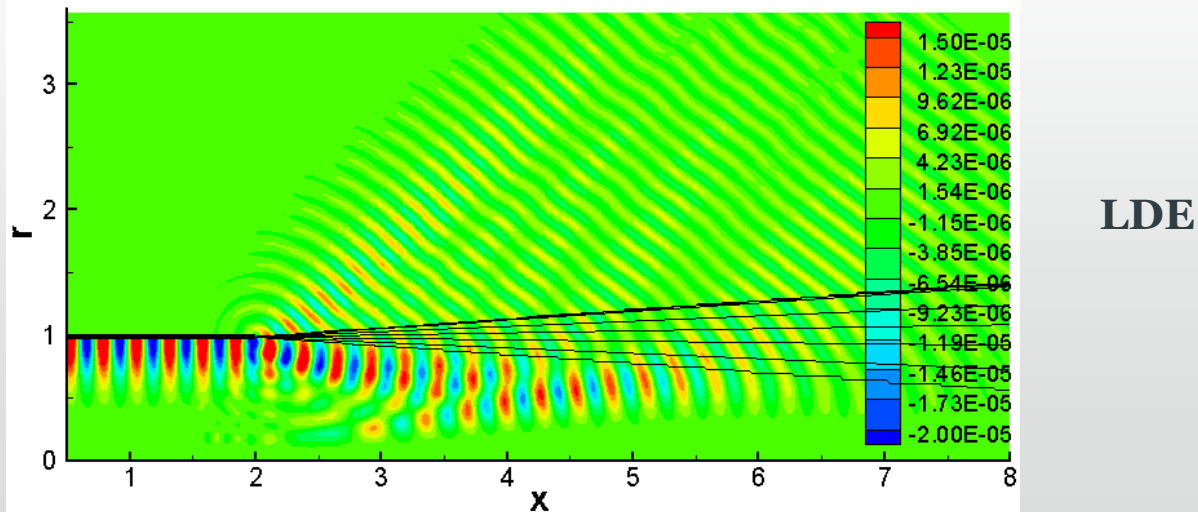
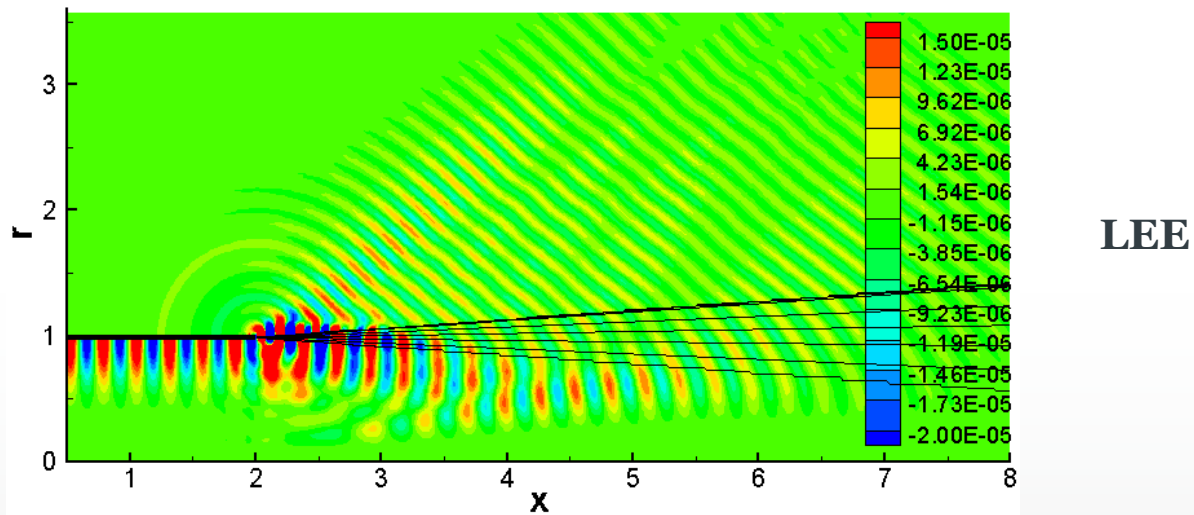
Further tests: linear shear layer

Mode (6,1), frequency = 1000Hz



Further tests: linear shear layer

Mode (6,1), frequency = 2000Hz



Comparison of computing time

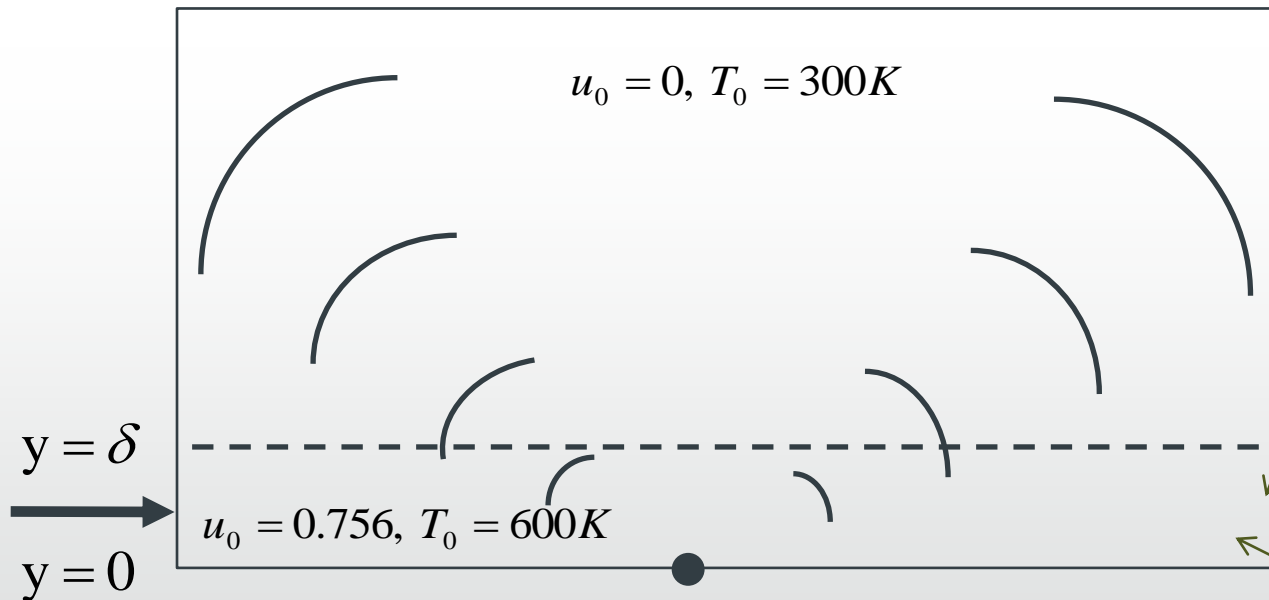
A PC was used with an E4500 Intel processor (2.2 GHz clock speed) and 2.0 Gigabytes of memory running on a 32-bit operating system

Model	Propagation Seconds per grid per time step	Computing time for 150 acoustic wave periods (minutes)
GTS	1.01×10^{-5}	230.1
GTF	1.23×10^{-5} (+23%)	281.9
LDE	1.77×10^{-5} (+75%)	403.7

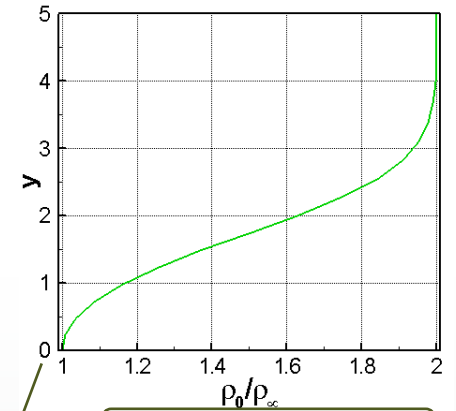
- For the case of a semi-infinite duct case, the computing time of the GTF method only increases 23% compared with GTS.
- LDE is the most expensive method.

CAA Benchmark Category 4, unstable jet

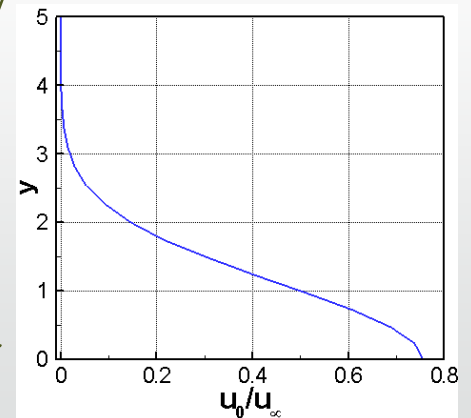
An source is placed inside the jet which has background velocity and density gradients



Acoustic source at $x=0, y=0$ with an excited frequency of 76 rad/s

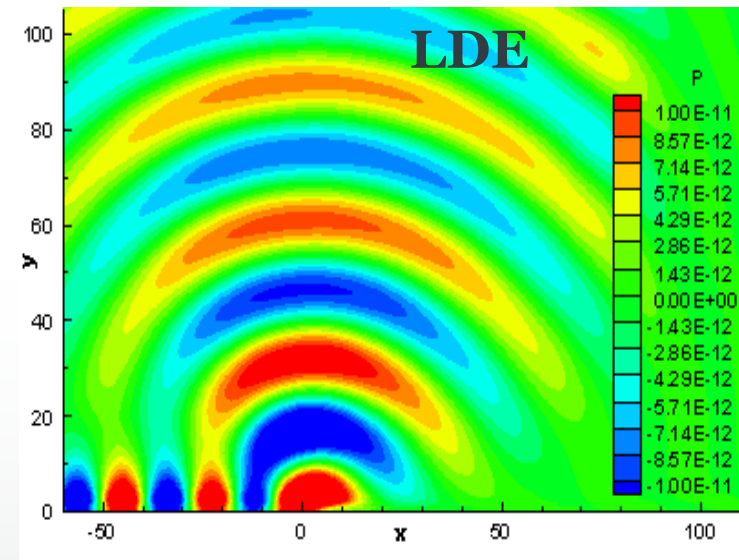
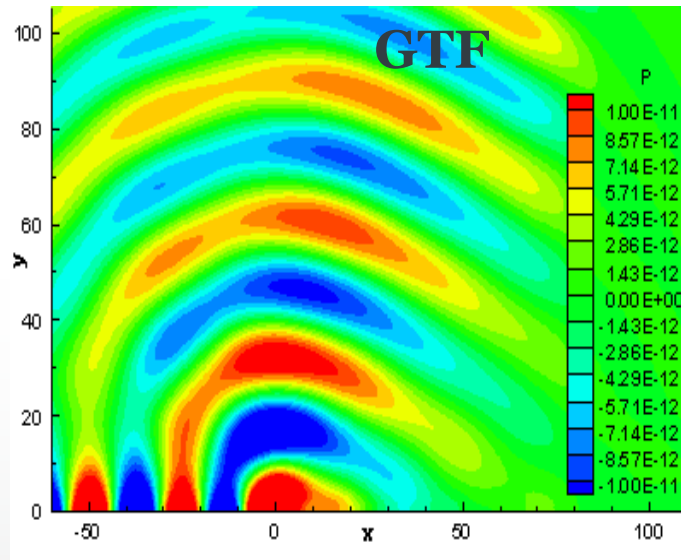


Density profile



u_0 profile

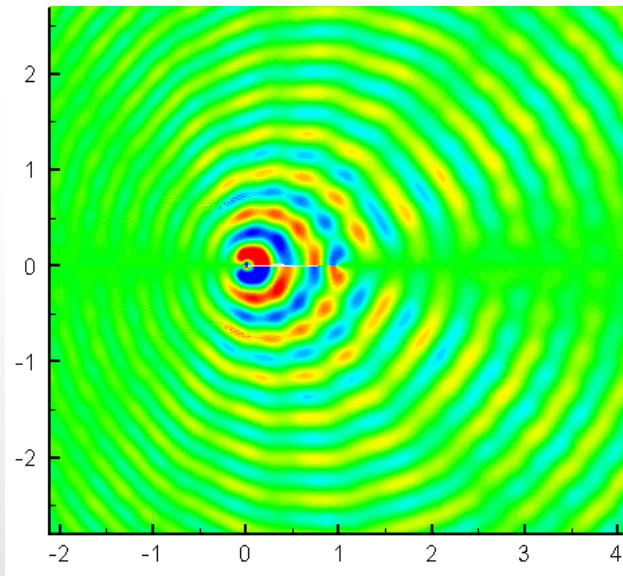
Pressure contours



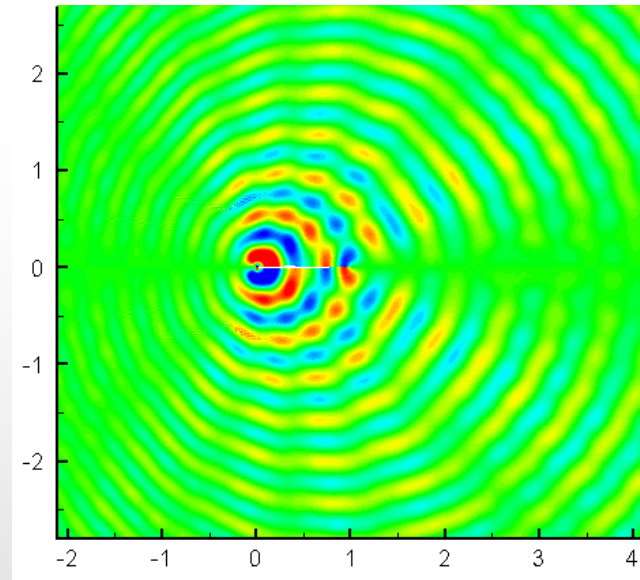
Vortical gust impinging on an airfoil

Near-field pressure contours

$M=0.3$
→

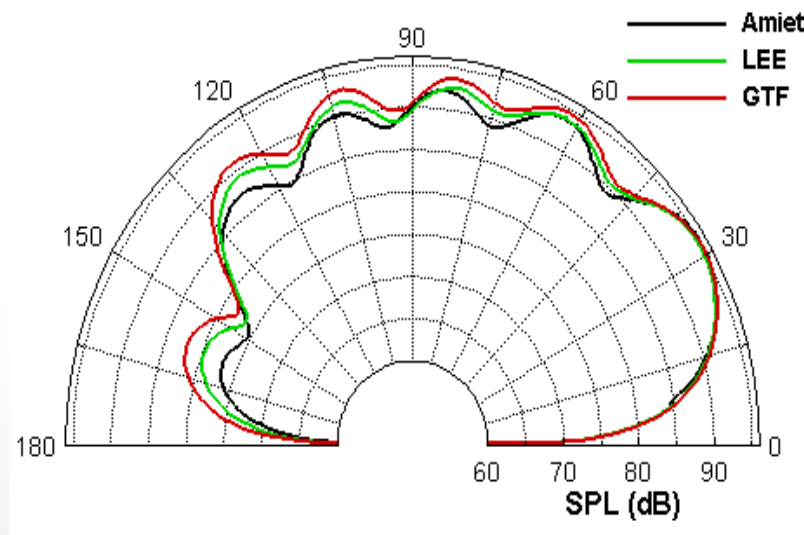


LEE



GTF

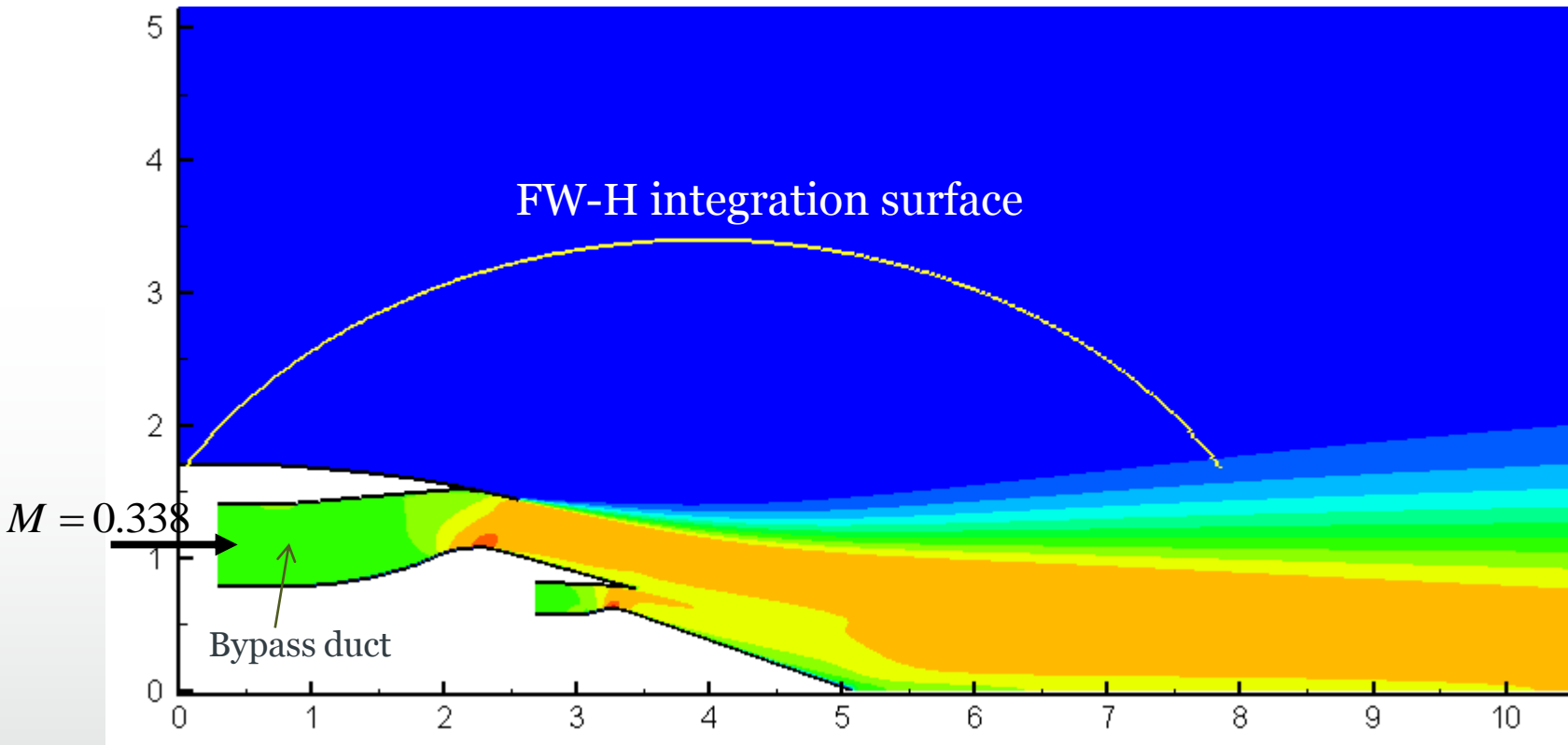
Vortical gust impinging on an airfoil



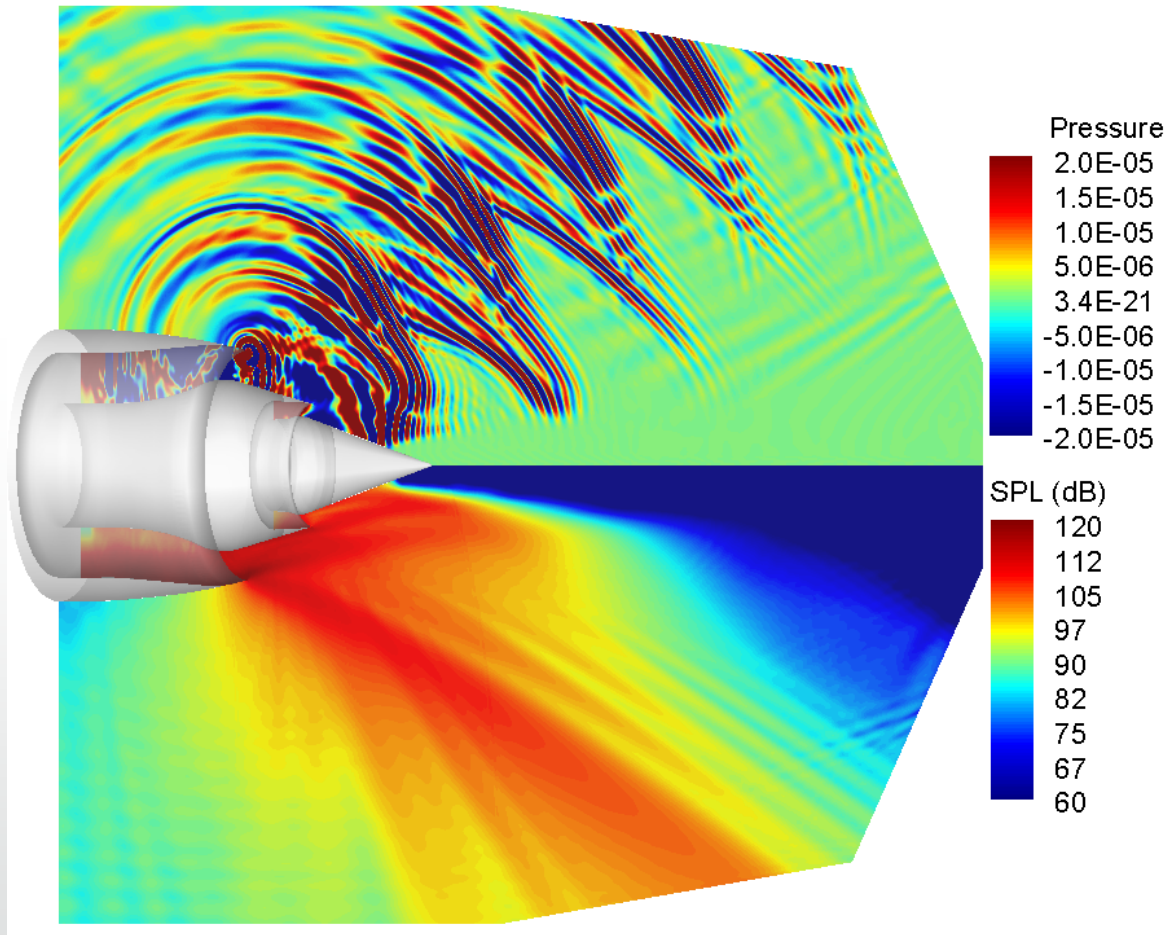
Far-field directivity

- GTF has the strongest prediction in both near and far-fields.
- This case shows that the GTF approach can model vortical waves.

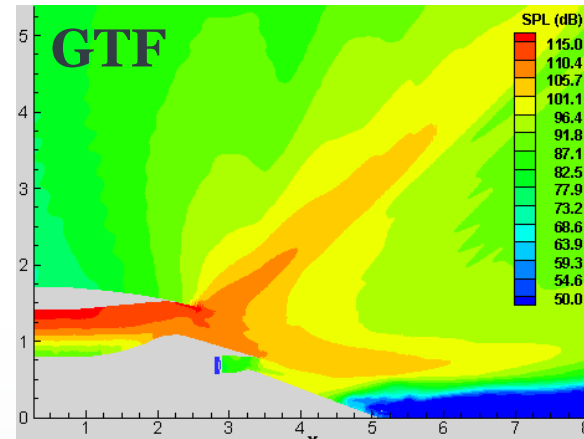
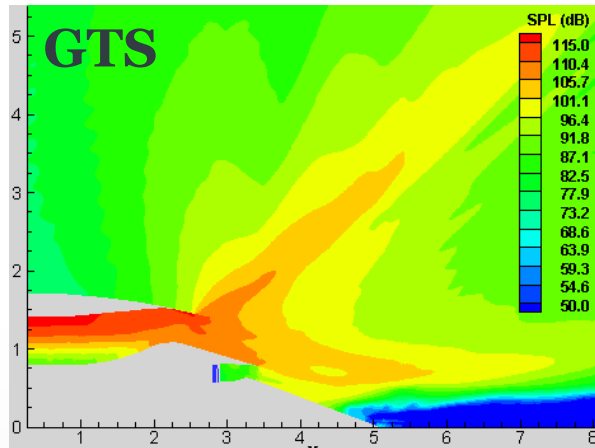
Application to engine: CFD mean flow



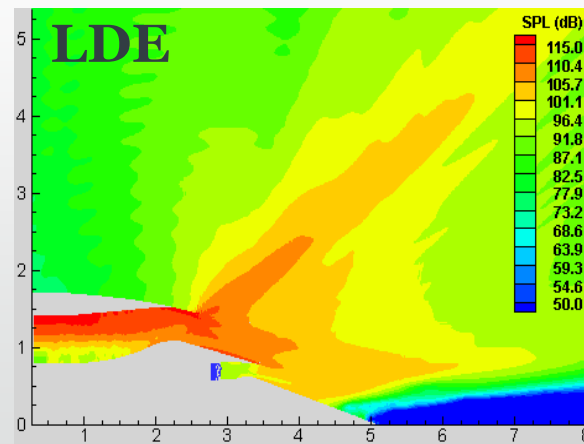
Mean flow Mach contour



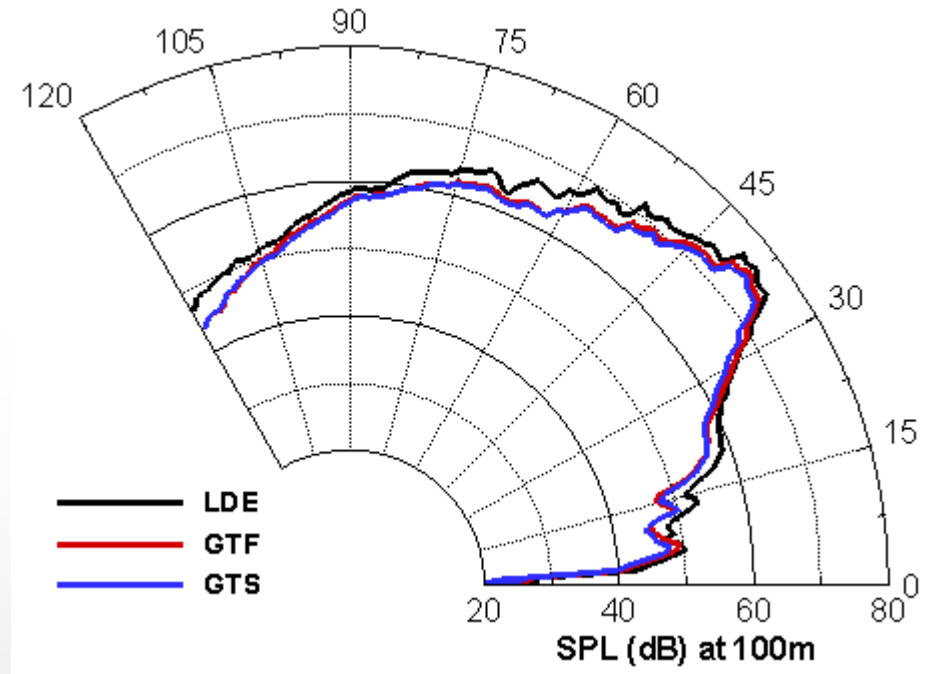
Application to engine: SPL



Mode $(m,n)=(13,1)$;
A combination of 18 frequencies :
200 to 3600Hz



Application to engine: CFD mean flow



Comparison of Far-field directivity

- Three methods have similar directivity pattern.
- LDE has the highest level of RMS (root-mean-square) pressure as it starts to show the unstable state observed in near-field.

Outlook

- Accurate, robust and efficient computation of propagation problems
- Broadband noise problems with synthesised turbulence
 1. Homogeneous, isotropic turbulence via a summation of discrete Fourier components
 2. Filtering random data
 3. Synthetic eddies
- Application to large, complex cases and account for the effects of scattering, diffraction, refraction, *etc.*

Summary

- Various linearised equations and treatment of LEE are developed, assessed and tested against a number of validation cases.
- These methods and equations are used to produce stable and efficient computation of sound propagation.
- We plan to extend the CAA methods to study broadband turbulence noise and complex problems.